Eur. Phys. J. D (2021) 75:302
https://doi.org/10.1140/epjd/s10053-021-00310-5

THE EUROPEAN PHYSICAL JOURNAL D

Regular Article – Atomic and Molecular Collisions

Molecular synthesis in ices triggered by dissociative electron attachment to carbon monoxide

Fabian Schmidt, Martin Philipp Mues, Jan Hendrik Bredehöft, and Petra Swiderek[a]

Fachbereich 2 (Chemistry/Biology), Institute for Applied and Physical Chemistry, University of Bremen, Leobener Straße 5, 28359 Bremen, Germany

Received 1 September 2021 / Accepted 10 November 2021 / Published online 2 December 2021

Abstract. Chemical reactions in mixed molecular ices as relevant in the context of astrochemistry can be initiated by electron-molecule interactions. Dissociative electron attachment (DEA) as initiating step is identified from the enhancement of product yields upon irradiation at particular electron energies. Herein, we show that DEA to CO leads to the formation of HCN in mixed CO/NH_3 ice at electron energies around 11 eV and 16 eV. We propose that this reaction proceeds via insertion of the neutral C fragment into a N–H bond. In the case of CO/H_2O and CO/CH_3OH ices, a resonant enhancement of the yields of HCOOH and CH_3OCHO, respectively, is observed around 10 eV. In both ices, both molecular constituents exhibit DEA processes in this energy range so that the energy-dependent product yield alone does not uniquely identify the relevant DEA channel. However, we demonstrate by comparing with earlier results on mixed ices where CO is replaced by C_2H_4 that DEA to CO is again responsible for the enhanced product formation. In this case, $O^{\cdot-}$ activates H_2O or CH_3OH which leads to the formation of larger products. We thus show that DEA to CO plays an important role in electron-induced syntheses in molecular ices.

1 Introduction

Electron-molecule interactions are typically associated with their dissociative nature which has been studied for many cases and reviewed repeatedly [1–8]. However, when these interactions occur in dense environments, reactive species resulting from such electron-induced dissociation can undergo further chemical reactions. This leads to the formation of new products [9–11] or can be exploited to fabricate novel materials with interesting properties [12,13]. Electron-induced chemical processes also receive attention with respect to research on the origin of organic molecules in space. It is nowadays recognized that low-energy electrons released under the effect of ionizing radiation can drive much of the interstellar chemistry within molecular ice layers that form on the surface of cold dust grains [11,14,15].

In fact, electron-molecule interactions can trigger reactions that lead to the synthesis of larger molecules from smaller building blocks. In ideal cases, the products can even incorporate all atoms of the initial reactants [16]. As prototypical examples, the syntheses of ethylamine ($C_2H_5NH_2$) from ethylene (C_2H_4) and ammonia (NH_3) [17], ethanol (C_2H_5OH) from ethylene (C_2H_4) and water (H_2O) [18], as well as formamide (H_2NCHO) from carbon monoxide (CO) and ammonia (NH_3) [19] have been observed under low-energy electron irradiation in cryogenic condensed ices containing the starting compounds. It was proposed in all three cases that electron ionization (EI) of one of the reactants creates an attractive force between adjacent molecules. This initiates a reaction sequence in which bonds form between the reactants, one of the hydrogen atoms migrates and the resulting product radical cation is neutralized by thermalized electrons thus leading to the neutral stable product.

While this ionization-driven reaction mechanism is temptingly simple, a deeper insight into the reactions occurring in the ice mixtures is of utmost importance to arrive at a comprehensive understanding of the electron-induced chemistry in ices. The potential complexity of the reaction networks is obvious considering the wealth of products that can be formed even in a pure ice as exemplified by the case of pure methanol (CH_3OH) ice [15,20]. As another example, ethanol (C_2H_5OH) formation was also observed as consequence of electron attachment (EA) to C_2H_4 in the presence of H_2O [18] indicating that different reaction mechanisms can contribute to the formation of a particular product.

In an effort to unravel electron-induced chemistry in ices, we have recently conducted comprehensive studies by post-irradiation thermal desorption spectrometry (TDS) on thin layers of different pure and mixed ices [20–23]. In each case, the dependence of product formation on electron energy was monitored for several products. This approach not only gives insight into the electron-molecule interactions that initiate the forma-

[a] e-mail: swiderek@uni-bremen.de (corresponding author)

tion of the products by releasing reactive intermediate species. It also allows us to draw conclusions on the reaction mechanisms that occur after this initial event. This is achieved by comparing the energy dependences of different products that are potentially formed via the same intermediates. Most interestingly, resonance structures around 10 eV in the energy dependences have suggested that dissociative electron attachment (DEA) to CO leads to formation of formic acid (HCOOH) in mixtures of CO and H_2O [22] and of methyl formate (CH_3OCHO) in mixed ices of CO and CH_3OH [23]. Here, we substantiate the claim that DEA to CO is an efficient pathway to product formation in ices. To this end, we present new results on mixed CO and NH_3 ices that reveal the role of DEA to CO in electron-induced chemistry by monitoring the formation of hydrogen cyanide HCN. Furthermore, we compare the results on CO/H_2O and CO/CH_3OH ices [22,23] with the data on mixed ices where CO is replaced by C_2H_4 [18,21] to demonstrate that a resonance around 10 eV is only visible when CO is present. We thus show that DEA to CO plays an important role in electron-induced syntheses in molecular ices and propose mechanisms for the reactions that are initiated by the fragments resulting from DEA.

2 Experimental

The electron energy-dependent formation of products upon electron irradiation of condensed molecular ices was monitored by post-irradiation thermal desorption spectrometry (TDS). The experimental procedures were described in detail previously [16–23]. Briefly, all experiments were performed in an ultrahigh vacuum chamber with a base pressure of 10^{-10} mbar. Molecular ices were prepared by leaking vapours of the reactants onto a Ta substrate (this work and Refs. [19–23]) or an Au substrate (Refs. [16–19]) held at $\sim$ 30–35 K either as a gas mixture or sequentially, the latter relying on rapid diffusion into pores of the first component. The amounts of gases leaked into the chamber were monitored as pressure drop in the gas handling manifold measured with an MKS Baratron type 622B capacitance manometer. Film thickness was estimated from TDS for the individual components by observing at which pressure drop the transition from monolayer to multilayer desorption signal occurs. TDS data were acquired by resistively heating the substrate with heating rates of $\sim$ 1 K/s while monitoring characteristic m/z ratios of the investigated neutral desorbing species using a quadrupole mass spectrometer (QMS) residual gas analyser (Stanford Research System RGA 200). The QMS has an electron-impact ion source operating at an electron energy of 70 eV.

The targeted mixing ratio of the two components in the ice can be established by different procedures. In the simplest case, a 1:1 gas mixture was leaked with the aim of producing an ice layer of the same composition. This procedure was applied previously for C_2H_4/NH_3 [17], C_2H_4/H_2O [18], as well as C_2H_4/CH_3OH [21] ices. The actual stochiometric ratio of the two reactants in the ice can be deduced by integrating the area under

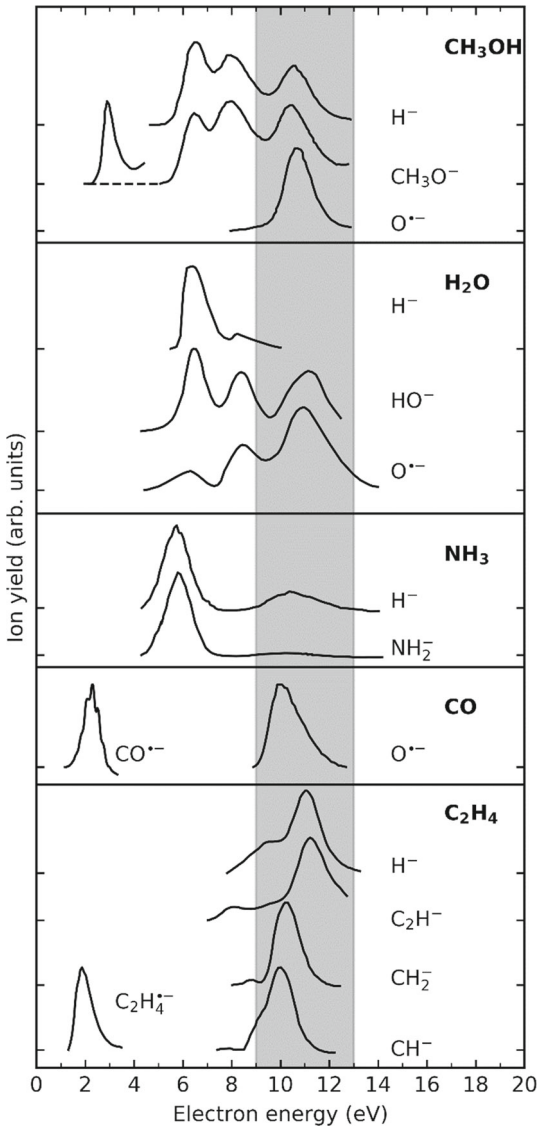

Fig. 1 Overview of gas phase dissociative electron attachment to CH_3OH (from Ref. [24] reporting DEA ion yields in arbitrary units), H_2O (from Ref. [25] reporting absolute DEA cross sections), NH_3 (from Ref. [26] reporting absolute DEA cross sections), CO (10 eV resonance from Ref. [27] reporting DEA ion yields in arbitrary units), and C_2H_4 (10 eV resonance from Refs. [28,29] reporting DEA ion yields in arbitrary units). In the case of C_2H_4, only the most intense signals are displayed. See Ref. [30] for data on minor fragments. Also included is non-dissociative electron attachment at 2 eV to CO (from Ref. [31] reporting charge trapping in arbitrary units) and C_2H_4 (from Ref. [32] derived from energy-dependent cross section for vibrational excitation). Each curve has been normalized to its maximum. The figure does not represent the relative yields of individual fragments from same molecule but merely serves to illustrate to resonance positions. Tick marks on the y-axis indicate the vertical offset

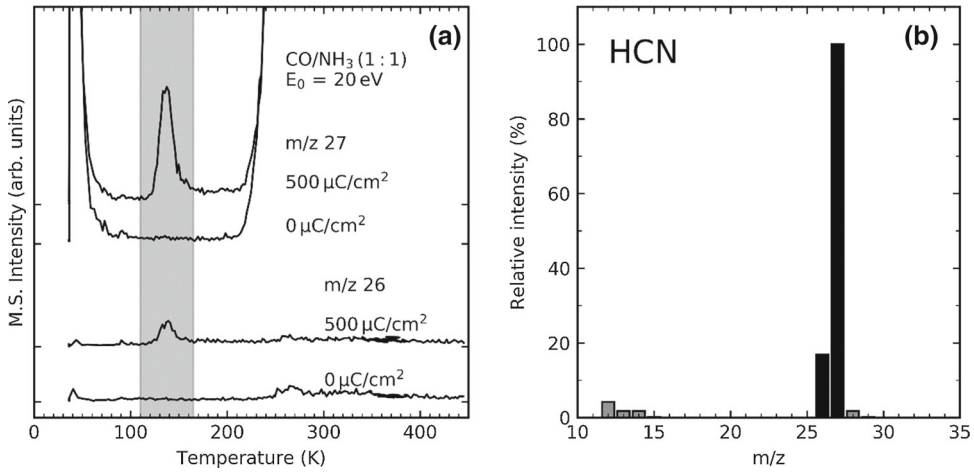

Fig. 2 **a** Thermal desorption spectra of CO/NH_3 mixed ice (thickness 10–14 monolayers) without electron exposure (denoted 0 $\mu C/cm^2$) and after electron irradiation with 500 $\mu C/cm^2$ at an electron energy (E_0) of 20 eV. The peaks at ∼133 K in the m/z 26 and 27 curves were assigned to HCN. The signals at ∼50 K and above 220 K in the m/z 27 curve result from desorption of CO from the ice and from parts of the sample holder that warm up more slowly than the Ta foil itself. CO is detected at m/z 27 due to its high abundance which leads to spillover of intensity to mass channels adjacent to the main signal at m/z 28. Tick marks on the vertical axis indicate the baseline level. **b** Reference mass spectrum of HCN [35]

the TDS curves and correcting for the partial electron ionization cross sections of the characteristic fragments that are monitored in the QMS [21]. The thus determined ice composition may deviate from the mixing ratio of the gases if one of the compounds adsorbs more strongly to the walls of the gas injection tube and to parts of the vacuum chamber than the other. In the case of C_2H_4/CH_3OH ice, the gas mixture was consequently adjusted to produce a 1:1 composition of the ice [21]. Alternatively, the two components can be leaked sequentially. This is advantageous when one component tends to form a porous ice such as H_2O. The pores can then accommodate the molecules of the subsequently dosed gas and this can enhance its sticking probability. This procedure was applied previously to prepare CO/H_2O ices [22] and also to study the formation of HCN in CO/NH_3 ices reported herein. In detail, the ice was prepared by leaking first an amount of NH_3 corresponding to a pressure drop of 28 mTorr in the manifold followed by CO (15 mTorr). According to TDS, this produced an ice with a comparable composition as used previously to investigate the formation of formamide [19].

Electron irradiation was performed using a commercial STAIB NEK-150-1 electron source with an energy resolution of 0.5 eV. After irradiation, the ice was desorbed in a TDS experiment, again with a heating rate of ∼ 1 K/s, while monitoring characteristic m/z ratios of the investigated neutral reaction products. After each experiment, the substrate temperature was held at 450 K for 2 min to desorb remaining species on the sample holder, which warms up more slowly than the substrate. A relative product yield was obtained by integrating the area under the characteristic desorption signals in the TDS curves. Typically, the same experiment was repeated three to four times to establish an experimental error. This overall procedure was then repeated for a range of electron energies to obtain energy-dependent product yields. Here, attention was paid to select an electron exposure that falls within the linear regime where product yields increase linearly with exposure. This ensures that the product yields obtained at different electron energies can be directly compared.

3 Results and discussion

3.1 DEA processes of the investigated molecular ice constituents

As a reference for the discussion of resonant product formation in the molecular ices studied herein, Fig. 1 provides an overview of the gas phase DEA processes of the individual ice components. It is well-established that the energetic position and the cross sections of the individual DEA channels can change in a condensed environment, the latter even by orders of magnitude [2,33]. Nonetheless, the overview given in Fig. 1 clearly illustrates the wealth of DEA processes that exist in the vicinity of 10 eV (grey band in Fig. 1). In fact, in both CO/H_2O and CO/CH_3OH mixed ices, both components exhibit DEA resonances around this energy. The position of the maximum product yield alone is therefore not a sufficient criterion to identify which DEA channel enhances the formation of a particular product in a mixed ice. Moreover, we note that electron-stimulated desorption of $O^{\cdot -}$ from condensed multilayer films of CO is reso-

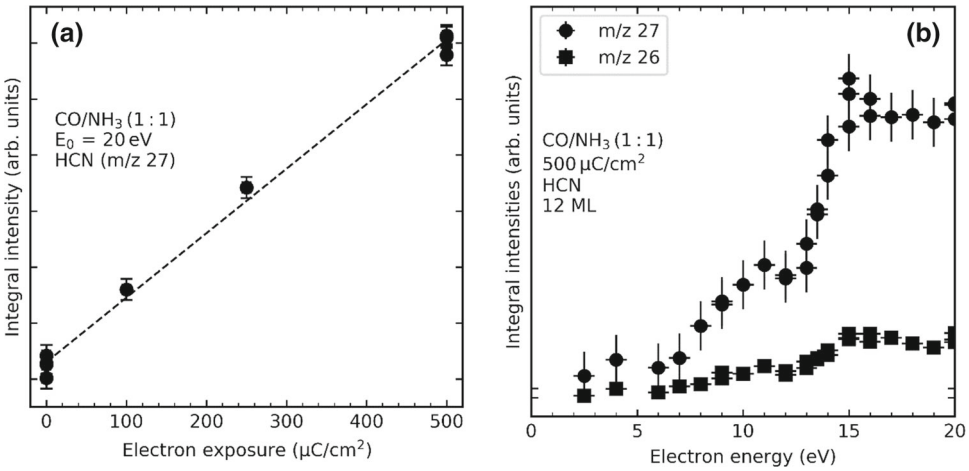

Fig. 3 **a** Peak areas for the m/z 27 desorption signal of HCN at 133 K obtained by TDS without electron exposure (plotted at 0 $\mu C/cm^2$) and after increasing electron irradiation of CO/NH_3 mixed ice at an electron energy (E_0) of 20 eV. Error bars denote the estimated error for the peak area. **b** Energy dependence of the relative yield of HCN formed after electron irradiation of CO/NH_3 ice with an electron dose of 500 $\mu C/cm^2$ as derived from the integrated m/z 27 and m/z 26 desorption signals. The thickness of the ice layer was 10–14 monolayers. Tick marks on the vertical axes indicate a peak area of zero

nantly enhanced around 12 eV [34,35] and thus about 2 eV above the maximum product yield in the mixed ices described above. Also, and in contrast to the gas phase, ESD from condensed CO evinces a second resonance around 16 eV [34,35]. We demonstrate in the following that these DEA channels indeed play a role in the investigated mixed ices. The neutral C fragment leads to the production of HCN in CO/NH_3 ice (Sect. 3.2) while the $O^{\cdot -}$ radical anion initiates both the formation of formic acid (HCOOH) in CO/H_2O ice and methyl formate (CH_3OCHO) in CO/CH_3OH ice (Sect. 3.3).

3.2 Molecular synthesis triggered by the neutral C fragment

The electron-induced chemistry of CO/NH_3 mixed ice has been investigated previously with particular focus on the formation of H_2NCHO [19]. A resonant enhancement of this product was observed in a broad range around 10 eV. Aiming at a more comprehensive insight, we have now investigated the production of HCN in CO/NH_3 ice and its dependence on the electron energy. Figure 2a shows representative TDS data obtained before and after electron irradiation at 20 eV. A distinct desorption signal with maximum at 133 K is seen in the TDS curves obtained for both m/z 26 and 27. The relative intensity of these signals is 1:5 and thus very similar to the intensity ratio of these two signals in a reference mass spectrum of HCN [36] (Fig. 2b) indicating that this product is indeed formed under electron irradiation of the CO/NH_3 ice.

To establish the relative product yields as function of electron energy, the area under the TDS signal at 133 K in the m/z 27 data was evaluated. First, it was verified that the exposure of 500 $\mu C/cm^2$ applied in Fig. 2a falls within the linear regime so that electron-induced depletion of the reactants CO and NH_3 as well as decomposition of the product HCN can still be neglected. Therefore, the integral intensity of the desorption signal was first plotted for increasing electron exposure at 20 eV (Fig. 3a). The product yield in fact increases linearly with electron exposure. As reaction rates are typically lower at lower electron energies, an electron exposure of 500 $\mu C/cm^2$ was thus also used in all subsequent experiments at lower electron energies. The resulting energy-dependent integral desorption signals of HCN are shown in Fig. 3b. The constant intensity ratio between the signals at m/z 27 and m/z 26 shows that the data are representative of HCN at all electron energies. The curves evince resonant enhancement of the product yield around 11 eV and 15 eV. DEA processes in NH_3 that could contribute to this enhancement have been reported around 10 eV (see Fig. 1) but not at higher energy. In contrast, apart from a shift to lower energy, the resonances observed here compare well with the maxima in the ESD yields of $O^{\cdot -}$ from condensed multilayer films of CO around 12 eV and 16 eV [34,35]. This shift is rationalized by considering that desorption of the anion requires a certain excess energy to overcome the polarization forces in the condensed phase. In contrast, HCN is produced within the layer and the energy required for desorption is supplied thermally in the subsequent TDS experiment. We thus conclude that DEA to CO is the initiating electron-molecule interaction that leads to the formation of HCN in the CO/NH_3 mixed ice. We propose that the neutral C fragment released together with $O^{\cdot -}$ upon DEA to CO reacts with NH_3 by insertion into one of the N-H bonds and subsequent elimination of H_2 to produce HCN (Fig. 4) as also reported earlier [37].

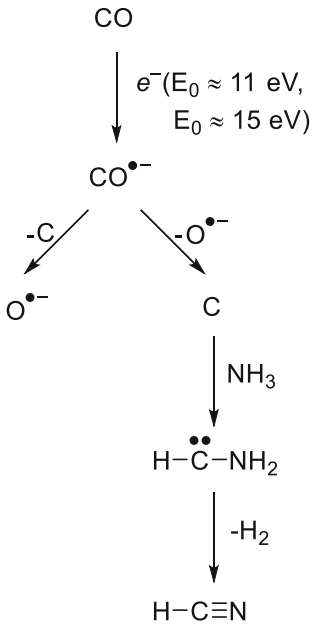

Fig. 4 Proposed reaction mechanism for the electron-induced formation of HCN in CO/NH_3 mixed ice

3.3 Molecular synthesis triggered by the $O^{\cdot -}$ radical anion fragment

Figure 5a shows the energy-dependent yield of HCOOH in mixed CO/H_2O ice [22] and Fig. 5b the yield of CH_3OCHO in CO/CH_3OH ice [23], both obtained from the areas under the characteristic TDS signals. For comparison, the data for ices in which CO is replaced by C_2H_4 [18,21] is also included. For details of the experiments and data analysis we refer to the previous studies [18,21–23]. The resonant enhancement of the yields of HCOOH and CH_3OCHO around 10 eV clearly indicates that an electron attachment process contributes to the product formation. We show now that the sequence of reactions leading to these products must be initiated by the $O^{\cdot -}$ radical anion resulting from DEA to CO. This is, however, not *a priori* obvious. In fact, both H_2O and CH_3OH also exhibit DEA channels in this energy range (Fig. 1). Furthermore, as discussed in Sect. 3.1, both the energies and the cross sections of DEA processes can change under the effect of the condensed medium.

The formation of HCOOH and CH_3OCHO through DEA must involve reactions of radical species with CO. This should be more favourable than reactions of negative ion fragments with the electron-rich CO molecule. Regarding HCOOH formation in CO/H_2O mixed ice, gas phase data suggest that DEA to H_2O around 10 eV produces either $O^{\cdot -}$ or OH^-, the latter accompanied by release of $H^{\cdot}$ (Fig. 1). In the mixed ice, $H^{\cdot}$ can react with CO to yield the $HCO^{\cdot}$ radical. This radical is a key intermediate to the formation of formaldehyde (H_2CO) as has also been deduced from the finding that H_2CO is resonantly formed around 4 eV [22] (see also Fig. 6). It was proposed that at this energy, the $HCO^{\cdot}$ radical results from electron attachment (EA) to CO yielding the $CO^{\cdot -}$ radical anion which in turn acts as a strong base and is thus converted to the $HCO^{\cdot}$ radical by transfer of a proton from H_2O. However, a corresponding resonant structure at 4 eV was not observed in the yield of HCOOH (Fig. 6) thus ruling out its formation by reaction of $HCO^{\cdot}$ with H_2O. Therefore, the DEA channel near 10 eV yielding OH^- and $H^{\cdot}$ cannot account for the 10 eV resonant signal in the yield of HCOOH (Fig. 5a, bottom and Fig. 6) and is also not dominant with respect to the formation of H_2CO (Fig. 6). In consequence, DEA yielding $O^{\cdot -}$ is the most conceivable reaction channel leading to HCOOH. $O^{\cdot -}$ can accept a proton from H_2O to yield $HO^{\cdot}$ which in turn can add to CO yielding a $HOCO^{\cdot}$ radical. The latter can react with further H_2O to yield the product HCOOH.

Having identified $O^{\cdot -}$ as the most likely species to initiate formation of HCOOH in CO/H_2O ice alone, however, does not provide a unique assignment of the DEA process that initiates the formation of HCOOH. In the gas phase, $O^{\cdot -}$ is produced both by DEA to CO around 10 eV and to H_2O at slightly higher energy (Fig. 1). Considering again that gas phase resonance energies can be shifted and cross sections modified in an ice layer [2,33], it was thus previously unclear which of these DEA processes drives the formation of HCOOH [22]. A comparison with the energy dependent yield of C_2H_5OH in mixed ices of C_2H_4 and H_2O [18] can resolve this question (Fig. 5a). The decisive step in the formation of C_2H_5OH is the addition of $HO^{\cdot}$ radicals to the double bond C_2H_4 [18]. As noted above, $HO^{\cdot}$ can be formed by reaction of $O^{\cdot -}$ with H_2O. However, a resonant enhancement around 10 eV is absent from the energy-dependent yield of C_2H_5OH (Fig. 5a, top). Instead, the yield of C_2H_5OH increases steadily above 8 eV (Fig. 5a) pointing to a process initiated by EI or possibly ND. Comparing the cases of CO/H_2O mixed ice with the C_2H_4/H_2O ice thus gives evidence that $O^{\cdot -}$ must be formed with much higher yield by DEA to CO than to H_2O in the mixed ice. In conclusion, DEA to CO is the initiating electron-molecule interaction that leads to formation of HCOOH in the CO/H_2O mixed ice. We note that C^- has also been observed in ESD from condensed multilayer films of CO but with yield peaking at 14 eV and thus about 2 eV higher than that of $O^{\cdot -}$ [34]. In contrast, the energetic shift between the maximum yield of HCOOH at 10 eV and the resonance position in ESD of $O^{\cdot -}$ is in line with the earlier conclusion that the ion needs about 2 eV excess energy to be able to desorb [34]. Therefore, we rule out a significant contribution of the resonance producing C^- to the formation of HCOOH around 10 eV seen in Figs. 5a and 6.

In the case of the CO/CH_3OH mixed ice [23], DEA channels of CH_3OH near 10 eV lead to H^- accompanied by $CH_3O^{\cdot}$ or fragments thereof, to CH_3O^- and $H^{\cdot}$, or to $O^{\cdot -}$ and corresponding neutral species (Fig. 1). Again, it is therefore not immediately obvious if DEA to CO or to CH_3OH triggers the resonant production of CH_3OCHO around 10 eV (Fig. 5b, top). A dominant contribution of the CH_3O^- and $H^{\cdot}$ DEA chan-

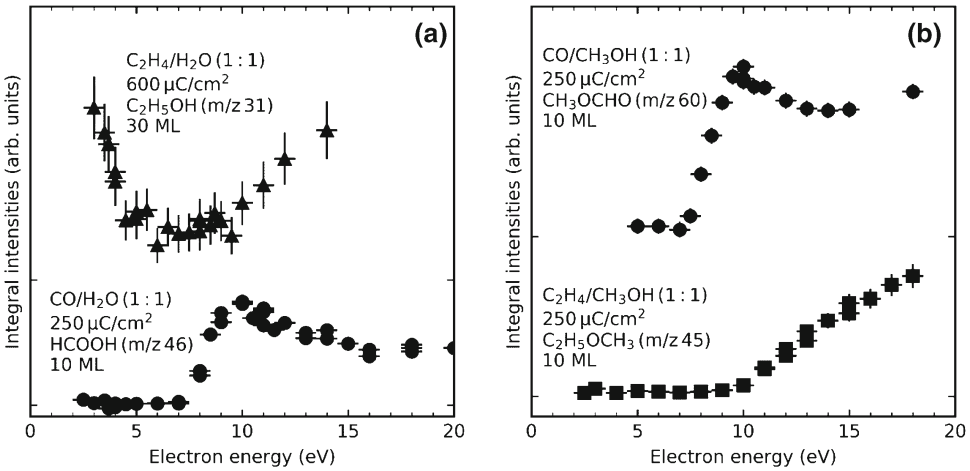

Fig. 5 Electron-energy dependent yields of product formation upon electron irradiation of different mixed ices: **a** HCOOH in CO/H_2O ice (bottom, from Ref. [22]) and C_2H_5OH in mixed C_2H_4/H_2O ice (top, from Ref. [18]), **b** CH_3OCHO in CO/CH_3OH ice (top, from Ref. [23]) and $C_2H_5OCH_3$ in C_2H_4/CH_3OH ice (bottom, from Ref. [21]). The thickness of the ice layers in monolayers (ML) is stated in the figures. In each set of experiments, the electron exposures were sufficiently small to ensure that the product formation increased linearly with exposure. Product yields at different energies thus reflect the relative values of the cross section for formation of each particular product. For details of the experiments see [18,21–23]

nel has been excluded. This was again deduced from the lack of resonant formation of the concurrent product H_2CO [23], anticipated to be produced by reaction of $H^{\cdot}$ with CO and subsequent abstraction of a hydrogen atom from CH_3OH by the resulting $HCO^{\cdot}$ radical. It is, however, more difficult to identify which of the remaining DEA channels is responsible for formation of CH_3OCHO. This product results when a $CH_3O^{\cdot}$ radical adds to CO to produce $CH_3OCO^{\cdot}$ which, in turn, abstracts a hydrogen atom from an adjacent CH_3OH molecule to yield the final product. $CH_3O^{\cdot}$ can result directly from DEA to CH_3OH or via reaction of $O^{\cdot -}$ with CH_3OH. Note again that $O^{\cdot -}$ is potentially formed by DEA to both CH_3OH and CO. These different reaction pathways can again be distinguished by comparing with the C_2H_4/CH_3OH mixed ice (Fig. 5b, bottom). Here, addition of $CH_3O^{\cdot}$ to C_2H_4 and abstraction of hydrogen from an adjacent molecule yields $CH_3OC_2H_5$ [21]. However, as deduced from the threshold-type behavior of the energy dependent product yield, this reaction is not dominated by DEA (see also [21]). In conclusion, this supports again that DEA to CO rather than DEA to CH_3OH is responsible for the 10 eV resonant enhancement of the yield of CH_3OCHO in CO/CH_3OH mixed ice (Fig. 5b, top). Overall, the comparison of different ice systems provides clear evidence that the $O^{\cdot -}$ DEA fragment from CO activates molecules such as H_2O and CH_3OH to initiate further chemical reactions. DEA to CO thus plays a dominant role in the electron-induced synthesis of larger products.

We finally comment on the different energetic position of the resonance maximum in the case of reactions driven by $O^{\cdot -}$ (10 eV) and the first maximum of the HCN production driven by the neutral C fragment (11 eV). It is possible that, in the latter case, the resonant process overlaps with contributions of ND and/or

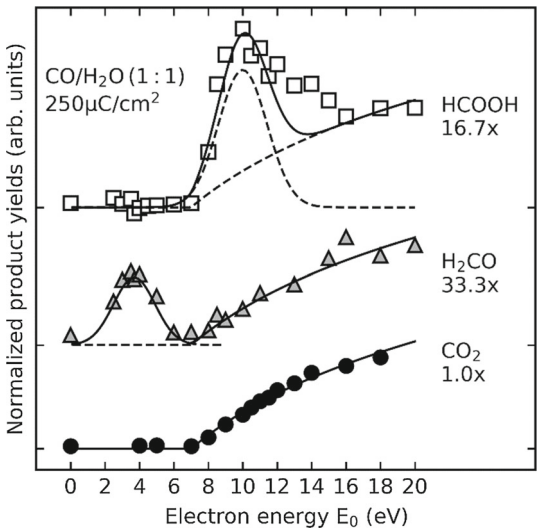

Fig. 6 Energy dependence of the relative yields of CO_2, HCOOH, and H_2CO formed after electron irradiation of mixed CO/H_2O ice with an electron dose of 250 $\mu C/cm^2$. Adapted with permission from Ref. [22]. Copyright 2019 American Chemical Society

DI that distort the DEA signal. As another explanation, the reactions initiated by $O^{\cdot -}$ and C may encounter differently high activation barriers. However, a comprehensive evaluation of this effect is beyond the scope of this work.

4 Conclusions

We have provided evidence that DEA to CO in mixed molecular ices is an important initiating electron-

molecule interaction leading to different reaction products. In the case of mixed CO/NH_3 ice, the neutral carbon fragment resulting from DEA to CO reacts with NH_3 to yield HCN. This is supported by the observed resonant enhancement of the HCN yield around 11 eV and 15 eV which is in good agreement with earlier ESD studies on condensed CO [34,35]. In CO/H_2O and CO/CH_3OH ices [22,23], the corresponding anionic DEA fragment $O^{\cdot-}$ initiates reactions leading to the formation of HCOOH and CH_3OCHO, respectively. This is evident from the comparison with mixed ices where CO is replaced by C_2H_4 [18,21]. In these latter systems, the 10 eV resonance seen in product formation in the ices containing CO is absent. We thus show that DEA to CO plays an important role in electron-induced syntheses in molecular ices. The understanding gained herein contributes to the general goal to unravel the reactions sequences in astrochemical molecular ices.

Acknowledgements The work presented here was funded by the Deutsche Forschungsgemeinschaft (DFG) under Project Number SW26/15-2.

Author contributions

FS performed the reevaluation of data for Sect. 3.3 and prepared Figs. 1, 2, 3 and 5, 6. MPM performed and analysed the experiments described in Sect. 3.2 and prepared Fig. 4. JHB supervised all experiments. PS wrote the manuscript. All authors have proof-read and discussed the final version of the manuscript.

Funding Open Access funding enabled and organized by Projekt DEAL.

Data availability statement This manuscript has no associated data or the data will not be deposited. [Authors' comment: The data sets generated during and/or analysed during the current study are available from the corresponding author upon request].

Declarations

Conflict of interest The authors declare no competing financial interest.

References

1. L.G. Christophorou, J.K. Olthoff, *Fundamental Electron Interactions with Plasma Processing Gases*, 1st edn. (Springer, Boston, 2004)
2. I. Bald, J. Langer, P. Tegeder, O. Ingólfsson, Int. J. Mass Spectrom. **277**, 4 (2008)
3. J.W. McConkey, C.P. Malone, P.V. Johnson, C. Winstead, V. McKoy, I. Kanik, Phys. Rep. **466**, 1 (2008)
4. C. Winstead, V. McKoy, Radiat. Phys. Chem. **77**, 1258 (2008)
5. J.H. Moore, P. Swiderek, S. Matejcik, M. Allan, in Nanofabrication Using Focused Ion and Electron Beams – Principles and Applications, edited by P. Russell, I. Utke, S. Moshkalev, 1st edn. (Oxford University Press, New York, 2012)
6. N.J. Mason, J. Phys.: Conf. Ser. **565**, 012001 (2014)
7. R.M. Thorman, T.P. Ragesh Kumar, D.H. Fairbrother, O. Ingólfsson, Beilstein J. Nanotechnol. **6**, 1904 (2015)
8. O. Ingólfsson, in Low-Energy Electrons: Fundamentals and Applications, edited by O. Ingólfsson, 1st edn. (Pan Stanford Publishing, Singapore, 2019)
9. A.D. Bass, L. Sanche, Low Temp. Phys. **29**, 202 (2003)
10. A. Lafosse, M. Bertin, R. Azria, Prog. Surf. Sci. **84**, 177 (2009)
11. C.R. Arumainayagam, H.-L. Lee, R.B. Nelson, D.R. Haines, R.P. Gunawardane, Surf. Sci. Rep. **65**, 1 (2010)
12. A. Turchanin, A. Gölzhäuser, Prog. Surf. Sci. **87**, 108 (2012)
13. A. Turchanin, Chimia **73**, 473 (2019)
14. M.C. Boyer, N. Rivas, A.A. Tran, C.A. Verish, C.R. Arumainayagam, Surf. Sci. **652**, 26 (2016)
15. C.R. Arumainayagam, R.T. Garrod, M.C. Boyer, A.K. Hay, S.T. Bao, J.S. Campbell, J. Wang, C.M. Nowak, M.R. Arumainayagam, P.J. Hodge, Chem. Soc. Rev. **48**, 2293 (2019)
16. E. Böhler, J. Warneke, P. Swiderek, Chem. Soc. Rev. **42**, 9219 (2013)
17. T. Hamann, E. Böhler, P. Swiderek, Angew. Chem. Int. Ed. **48**, 4643 (2009)
18. J. Warneke, Z. Wang, P. Swiderek, J.H. Bredehöft, Angew. Chem. Int. Ed. **54**, 4397 (2015)
19. J.H.Bredehöft, E.Böhler, F. Schmidt T. Borrmann, P. Swiderek, ACS Earth Space Chem. **1**, 50 (2017)
20. F. Schmidt, P. Swiderek, J.H. Bredehöft, ASC Earth Space Chem. **5**, 391 (2021)
21. F. Schmidt, P. Swiderek, J.H. Bredehöft, J. Phys. Chem. A **123**, 37 (2019)
22. F. Schmidt, P. Swiderek, J.H. Bredehöft, ASC Earth Space Chem. **3**, 1974 (2019)
23. F. Schmidt, P. Swiderek, T. Scheele, J.H. Bredehöft, Phys. Chem. Chem. Phys. **23**, 11649 (2021)
24. B.C. Ibanescu, O. May, A. Monney, M. Allan, Phys. Chem. Chem. Phys. **9**, 3163 (2007)
25. Y. Itikawa, N. Mason, J. Phys. Chem. Ref. Data **34**, 1 (2005)
26. P. Rawat, V.S. Prabhudesai, M.A. Rahman, N.B. Ram, E. Krishnakumar, Int. J. Mass Spectrom. **277**, 96 (2008)

27. K. Gope, V. Tadsare, V.S. Prabhudesai, N.J. Mason, E. Krishnakumar, Eur. Phys. J. D **70**, 134 (2016)
28. J.C.J. Thynne, K.A.G. MacNeil, J. Phys. Chem. **75**, 2584 (1971)
29. L. von Trepka, H. Neuert, Z. Naturforsch. A: Phys. Sci. **18**, 1295 (1963)
30. E. Szymańska, N.J. Mason, E. Krishnakumar, C. Matias, A. Mauracher, P. Scheier, S. Denifl, Int. J. Mass Spectrom. **365–366**, 356 (2014)
31. R.D. Rempt, Phys. Rev. Lett. **22**, 1034 (1969)
32. I.C. Walker, A. Stamatovic, S.F. Wong, J. Chem. Phys. **69**, 5532 (1978)
33. A.D. Bass, L. Sanche, Radiat. Environ. Biophys. **37**, 243 (1998)
34. L. Sanche, Phys. Rev. Lett. **53**, 1638 (1984)
35. R. Azria, L. Parenteau, L. Sanche, J. Chem. Phys. **88**, 5166 (1988)
36. NIST Mass Spectrometry Data Center, W. E. Wallace, director, in NIST Chem. WebBook, NIST Stand. Ref. Database Number 69, Eds. P.J. Linstrom W.G. Mallard, Gaithersburg MD, 20899, https://doi.org/10.18434/T4D303 (retrieved March 13, 2020)
37. P.B. Shevlin, D.W. McPherson, P. Melius, J. Am. Chem. Soc. **105**, 488 (1983)